Virology 537 (2019) 237–245

Contents lists available at ScienceDirect

Virology

journal homepage: www.elsevier.com/locate/virology

Extensive genomic recoding by codon-pair deoptimization selective for mammals is a flexible tool to generate attenuated vaccine candidates for dengue virus 2

Charles B. Stauft[a,1,2], Yutong Song[a,2], Oleksandr Gorbatsevych[a], Petraleigh Pantoja[b], Idia V. Rodriguez[b], Bruce Futcher[a], Carlos A. Sariol[b], Eckard Wimmer[a,*]

[a] Department of Molecular Genetics and Microbiology, Stony Brook University School of Medicine, Stony Brook, NY, USA
[b] Unit of Comparative Medicine, Virology Laboratory, Caribbean Primate Research Center, University of Puerto Rico, San Juan, PR, USA

ARTICLE INFO

Keywords:
Vaccine
Dengue virus
Antibody-dependent enhancement
Rhesus macaques
Codon-pair-bias
Codon usage
Arbovirus
Zika virus

ABSTRACT

The four serotypes of dengue virus (DENV) are the leading etiologic agent of disease caused by arthropod-borne viruses (arboviruses) in the world, with billions at risk of DENV infection spread by infected mosquitoes. DENV causes illness ranging from dengue fever (DF) to life-threatening dengue hemorrhagic fever (DHF) and dengue shock syndrome (DSS). DENV proliferates well in two different host systems, an invertebrate mosquito vector and vertebrate primate host, which have a distinct difference in their preference of codon *pairs* (CP) for translation (different "*codon pair bias*"). Consequently, arboviruses must delicately balance the use of codon pairs between mammals and arthropods, which presents an *Achilles' heel* that we have exploited by specifically shifting the codon pair preference in the E and NS3 ORFs away from mammals while keeping the CPB favorable for mosquito ORFs. Here we report that recoding of the ORFs has led to variants that were *over-attenuated* in rhesus macaques although induction of protective antibodies in animals vaccinated with the smallest recoded ORF (E) was observed. The flexibility of our synthetic vaccine design (by decreasing the number of unfavorable CPs in the E ORF), allowed us to construct two new vaccine candidates (E^{hminA} and E^{hminB}) with intermediate attenuation in cell culture and neonatal mice, a result demonstrating proof of concept. New DENV vaccine candidates are being developed based on selective attenuation by dramatic recoding, with flexibility in balancing the attenuation and immunogenicity by marrying rational design and empirical modification.

1. Introduction

Flaviviruses such as dengue virus (DENV), Zika virus (ZIKV), and yellow fever virus (YFV) are pathogens of great international public health concern. Billions of humans throughout the tropics and subtropics are at risk of infection, and thousands are killed each year (Lindenbach et al., n.d.; Pierson and Diamond, n.d.). Vaccine development against the four serotypes of DENV faces daunting obstacles but we have developed a unique approach of recoding DENV by modifying specifically their mammalian *codon-**pair**-bias*, thereby creating live-attenuated DENV2 vaccine candidates, a strategy we have dubbed SAVE (Coleman et al., 2008).

Gene expression by translation follows two functionally very different "rules": the well-known "codon bias" and the widely ignored "codon *pair* bias". The first is the unequal use of synonymous codons for a single amino acid. For example, in mammals the codon GUG for Val is used far more often used than the synonymous codon GUU. The second "rule" describes the observation that ***pairs*** of synonymous codons do not appear in mRNAs of species X at the frequency one would predict based on the genome-wide "codon usage." That is, a highly used codon within the cocktail of synonymous codons may not appear in codon *pairs* with the frequency expected from the frequency of its individual usage. It is now recognized that **codon pair bias (CPB)** is a fundamental property observed in all known taxa. It was first described by

* Corresponding author.
E-mail addresses: charles.stauft@stonybrook.edu (C.B. Stauft), yutong.song@stonybrook.edu (Y. Song), oleksandr.gorbatsevych@stonybrook.edu (O. Gorbatsevych), petraleigh.pantoja@upr.edu (P. Pantoja), idia.rodriguez1@upr.edu (I.V. Rodriguez), bruce.futcher@stonybrook.edu (B. Futcher), carlos.sariol1@upr.edu (C.A. Sariol), eckard.wimmer@stonybrook.edu (E. Wimmer).
[1] Present Affiliation: Codagenix Inc., Melville, New York, United States of America.
[2] CBS and YS contributed equally to this work.

https://doi.org/10.1016/j.virol.2019.09.003
Received 12 May 2019; Received in revised form 2 September 2019; Accepted 3 September 2019
Available online 05 September 2019
0042-6822/

Goodman and Hatfield in 1989 (Gutman and Hatfield, 1989) but its importance was not immediately appreciated. The whole genome synthesis of poliovirus (Cello et al., 2002) allowed subsequent investigations of the genetics, codon pair bias included, and pathology of recoded RNA viruses that was hitherto not possible (Coleman et al., 2008; Le Nouën et al., 2014; Mueller et al., 2006, 2005; Song et al., 2017).

We searched thousands of ORFs of the human genome and found that some codon pairs are (unexpectedly) overrepresented while others are (unexpectedly) underrepresented (Coleman et al., 2008). We correctly guessed that the overrepresented codon pairs serve well in expressing biological function (good pairs) in contrast to the underrepresented (bad pairs)(Coleman et al., 2008). We have quantified over- and underrepresentation of codon pairs by defining a "codon pair score" (CPS). This is the natural logarithm of the ratio of the observed frequency of the codon pair to the expected frequency of the pair (i.e., CPS = ln (Observed/Expected)(Coleman et al., 2008). "Expected" is based on the actual occurrences of codons taking into account codon usage. Over-represented codon pairs have a positive CPS score (+CPS) and they are favorable ("good") for ORF expression whereas the underrepresented have a negative CPS (-CPS) and they are unfavorable (bad) for ORF expression (Coleman et al., 2008).

The biological consequence in ORF expression of a single + CPS codon pair vs a single –CPS codon pair is very small. Single good or bad codon pairs are usually ignored by the translational machinery. But recoding a viral ORF with predominantly –CPS codon pairs can be catastrophic and will kill the virus. We have shown this in our early work with poliovirus Coleman et al., 2008. We synthesized a poliovirus genome such that the capsid coding region contained hundreds of bad codon pairs (a process we call "codon pair deoptimized", CPD) (Coleman et al., 2008). This construct was non-viable in spite of the fact that no amino acid changes had been introduced and the same codon usage was retained (Coleman et al., 2008). Meanwhile,it has been reported that proliferation of *every* RNA virus and some DNA viruses studied so far is crippled as result of increasing –CPS (bad) codon pairs beyond a threshold (Broadbent et al., 2016; Conrad et al., 2018; Diaz-San Segundo et al., 2015; Eschke et al., 2018; Le Nouën et al., 2014; Li et al., 2018; Martrus et al., 2013; Ni et al., 2014; Shen et al., 2015; Wang et al., 2015; Yang et al., 2013). Importantly, we can adjust the degree of codon pair deoptimization, e.g. we can decide by computer-aided design to increase the number of "bad" codons, e.g. the extent of the attenuation. Selective recoding hundreds of synonymous nucleotides allows flexibility in balancing attenuation and immunogenicity when combined with rational design and empirical modification.

We recently observed that the CPB of mammals differs significantly from that of mosquitoes (Fig. 1A vs 1B) (Shen et al., 2015; Stauft et al., 2018). For example, the CPS for the codon pair GCG-GGC (Ala-Gly) is +0.655 in mammals and −0.651 in mosquitoes (Shen et al., 2015). The difference in CPB in mammals (humans) versus mosquitoes presents an *Achilles' heel* for arboviruses that we have exploited by specifically shifting the codon pair preference in a DENV2 ORF away from mammals while keeping the codon pairs favorable for mosquito ORFs (Fig. 1) (Shen et al., 2015; Stauft et al., 2018).

Specifically, we deoptimized individually the sequences for DENV2 E and NS3 with respect to human preference, while maintaining mosquito preference. These recoded seqments are called E^{hmin}, $NS3^{hmin}$, and $NS5^{hmin}$ in Fig. 1A and Table 1. Fig. 1B depicts the drastic changes of codon pair scores of these three DENV proteins E and NS3 after CPD to negative values relative to mammalian codon pair bias. In contrast, the average scores remain unchanged relative to insect codon pair bias (Fig. 1C). Note that CPD alters the nt sequence of the coding region of the entire E glycoprotein in the DENV E^{hmin} variant as indicated in Table 1. We have shown that the new nucleotide sequence of E has only a very small, if any, effect on the E function in insect cells but a drastic effect of the E on the function in the mammalian cells (Shen et al., 2015; Stauft et al., 2018).

2. Materials and methods

2.1. Generation of recoded dengue virus variants

$DENV2^{syn}$, E^{hmin}, and $NS3^{hmin}$ were generated from synthetic viral cDNA as described previously (Shen et al., 2015). Based on our previous E^{hmin} construct, we further shortened the CPD regions within E^{hmin} to generate two separated de-attenuated DENV2 E^{hminA} and E^{hminB} variants. We employed two strategies in parallel to produce either target infectious clones or PCR-based RNA templates.

By using standard molecular techniques, we split the old E^{hmin} recoded sequences into two parts. The first half recoded fragment is named E^{hminA}, which contains CPD sequences in nucleotide position between 940 and 1674 (735 nt), whereas the second half recoded section is named E^{hminB} that has CPD sequences between 1681 and 2421 (741 nt). The re-encoded regions were inserted into the *Mlu I - Afl II* (DENV2 $E^{hminA/B}$) sites of the pBR322 $DENV2^{syn}$ backbone by ligation, and eventually transformed into DH5-α cells. This was used to generate the E^{hminA} and E^{hmin} recoded RNA templates as they were refractory to growth in NEB competent *E. coli*. The constructs were verified by sequencing, linearized with *Xba I*, transcribed with the phi-2.5 T7 promoter using T7 high yield transcription kit (NEB) in the presence of the m^7GpppA RNA cap structure analog (NEB). After a 3-h reaction at 37 °C, template DNA was digested with RNase-free DNase I and RNA were purified by precipitation with RNeasy Kit (Qiagen). The concentration of *in vitro* transcribed RNA was determined with a NanoDrop spectrophotometer (Thermo Scientific) and its integrity was checked by agarose gel electrophoresis. BHK-21 cells were electroporated with ~1 μg of RNA using Bio-Rad electroporator Gene Pulser Xcell Total System according to the manufacturer's instructions. Electroporated cells were plated in 6-well plate and incubated at 37 °C in the same medium used for DENV infection experiments.

2.2. Cell and virus culture

Vero E6 (CCL-81) cells and LLC-MK2 cells (CCL-7) were acquired from the American Type Tissue Culture collection (ATCC, Manassas VA) and grown in Modified Eagle's Medium (MEM) supplemented with 10% fetal bovine serum (FBS; Gemclone) and Penicillin/Streptomycin (CellGro). Primate cells were maintained at 5% CO_2 and 37 °C.

C6/36 cells (CRL-1660) were acquired from the ATCC (Manassas VA) and grown in Modified Eagle's Medium (MEM) supplemented with 10% FBS, 1% non-essential amino acids (NEAA; Gibco), and 1x Penicillin/Streptomycin. C6/36 cells were incubated at 28 °C and 5% CO_2.

Following generation of live virus using transfection of BHK-21 (CCL-10) cells, acquired from the ATCC (Manassas VA), each recoded variant was grown in C6/36 cells at a MOI of 1.0 for 7 days to generate stocks for use in subsequent experiments.

2.3. Focus forming assays

To count infectious virus particles, samples were added to confluent Vero or C6/36 cell monolayers in a 12-well format with a volume of 100 μL. Plates were rocked at room temperature for 30 min, then 400 μL of additional Vero infection medium (MEM supplemented with 5% FBS and Penicillin/Streptomycin) was added and the plates incubated at 37 °C (Vero) or 28 °C (C6/36), 5% CO_2 for 1 h. Medium was then aspirated from each plate, the wells were washed once with sterile DPBS, and 1 mL of 0.6% Tragacanth Gum, 5% FBS MEM was added to each well. The plates were incubated at 37 °C, 5% CO_2 for 5 (Vero) or 3 (C6/36) days before being fixed with 100% methanol and stained with HRP conjugated 4G2 anti-envelope antibody and a Vector VIP HRP staining kit (Vector Laboratories, Inc., Burlingame, CA). The limit of detection on the focus forming assays was 10 FFU/mL.

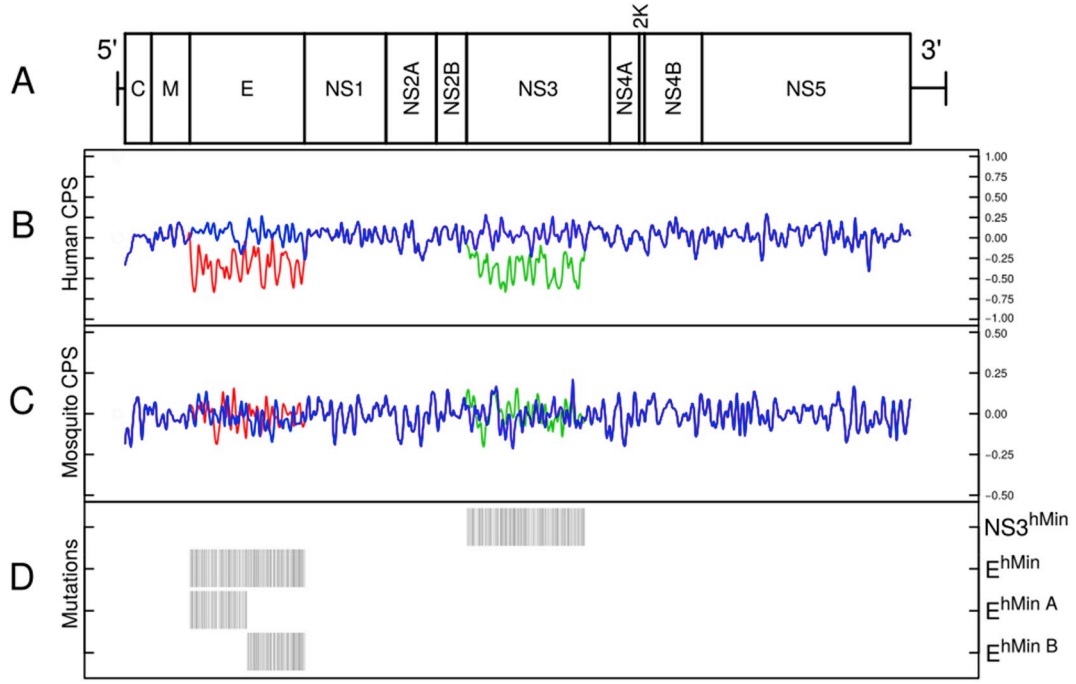

Fig. 1. Diagram of DENV2^{syn}, E^{hmin}, E^{hminA}, E^{hminB} and NS3^{hmin}. (*A*) Diagram of the DENV2 genome marks the polyprotein coding region and the coding regions of polypeptides before proteolytic processing. The color-coded lines indicate regions recoded in the three *hmin* viruses in the two CPS line plots show how the codon pair score changes along the length of the genome for each virus relative to the (B) human and (C) mosquito (*Aedes aegypti*) codon pair bias. There are three overlapping loess curves: E^{hmin} is in red, NS3^{hmin} is in green, and DENV2^{syn} is in blue. (D) Full length genomes of the four *hmin* viruses (NS3^{hmin}, E^{hmin}, E^{hminA}, E^{hminB}) are aligned to the WT (DENV2^{syn}) sequence, and point mutations generated by codon pair recoding are indicated by a barcode diagram.

2.4. Detection of neutralizing antibody by focus-reduction-neutralization 50% assay

Macaque serum was collected and analyzed by a focus reduction neutralization 50% ($FRNT_{50}$) assay to detect neutralizing antibodies. Briefly, sera were heat treated for 30 min at 56 °C and then incubated at 37 °C for 1 h with 50 FFU of DENV2^{syn} or DENV2 NGC-44 before being used to infect Vero E6 cells. The cells were incubated at 37 °C for 5 days and then stained using 4G2 primary anti-E glycoprotein antibody (Sigma-Aldrich), anti-mouse secondary IgG (Sigma-Aldrich), and Vector VIP reagent (Vector Laboratories). The serum was tested at two-fold dilutions and the $FRNT_{50}$ value given as the reciprocal of the highest dilution of serum neutralizing at least 50% of DENV2^{syn} virus.

2.5. Attenuation experiments in mice

To measure the attenuation of our DENV2 constructs, neonatal (1–2 day old) Swiss Webster mice (Charles River) were injected by the intracranial route with ten-fold serial doses of each recoded virus and synthetic wild-type virus diluted in infection medium at a total volume of 20 µL. Mice were checked for morbidity (clinical signs, weight loss) and mortality twice daily for 28 days post-injection. Humane early endpoints such as hind limb paralysis, sick rodent posture, tremor, low weight, and hunching were used in lieu of mortality. The doses used for DENV2^{syn} were 100 (n = 6), 10^1 (n = 7), and 10^2 (n = 6) FFU of which all mice at the 10^1 and 10^2 FFU dose were euthanized due to low weight and hunched rodent posture by trained personnel using decapitation with a sharp scalpel in order to avoid contamination of brain tissue (Leary et al., 2013). A very low dose (1 FFU) was used for DENV2^{syn} due to the low LD_{50} observed in our previous study using a different newborn mouse model (Shen et al., 2015). The doses used for E^{hmin} were 10^3 (n = 12), 10^4 (n = 5), and 10^5 (n = 5) FFU of which 1 mouse was found dead and 15 euthanized by decapitation due to appearance of tremor and hunching. The doses used for E^{hminA} were 10^1 (n = 6), 10^2 (n = 7), and 10^3 (n = 5) FFU of which one mouse was found dead, and 14 euthanized early due to appearance of clinical signs (paralysis). The doses used for E^{hminB} were 10^1 (n = 10), 10^2 (n = 10), and 10^3 (n = 5) FFU of which 13 were euthanized early due to the appearance of clinical signs, none were found dead. A single dose of 10^3 was used for NS3^{hmin} (n = 6) as an over-attenuated control of which only 1 mouse was euthanized early to the appearance of clinical signs, none were found dead. Surviving mice were allowed to reach 28 days of age and euthanized by CO_2 inhalation.

Table 1
Codon pair scores of individual coding regions of DENV2^{syn} after codon pair-deoptimization and nucleotide changes resulting from recoding.

Region	Encoding	Length (nt)	Δ (NT)	Mosquito CPS	Human CPS	C_3G_1
E	WT	1485		−0.022	0.055	7
E	hmin	1485	334/1485 (22%)	−0.018	−0.360	75
E^A	WT	735		0.007	0.050	4
E^A	hmin	735	156/735 (21%)	−0.006	−0.360	39
E^B	WT	741		−0.052	0.065	3
E^B	hmin	741	178/741 (24%)	−0.008	−0.340	36
NS3	WT	1854		−0.015	0.048	20
NS3	hmin	1854	402/1854 (22%)	−0.015	−0.360	86

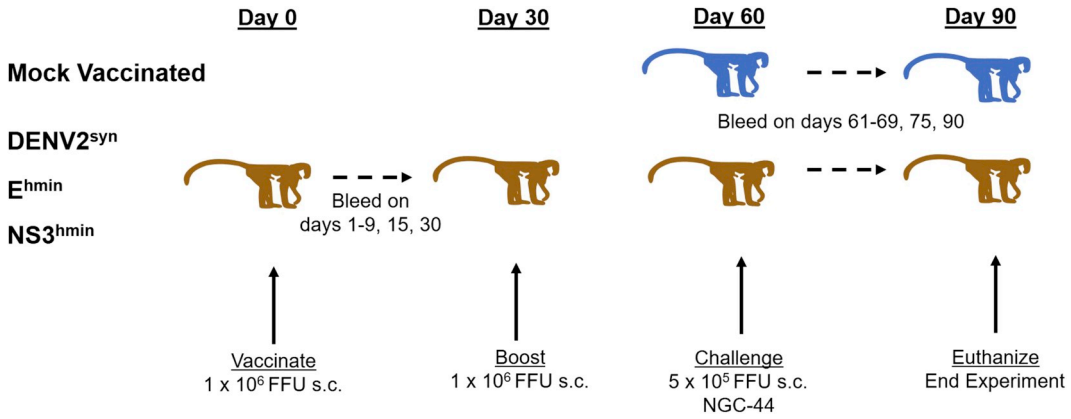

Fig. 2. Experimental design for macaque vaccination with DENV2^{syn}, E^{hmin}, and NS3^{hmin}. Rhesus macaques (n = 6) were either mock vaccinated with virus diluent, or given 10^6 FFU of DENV2^{syn}, E^{hmin}, or NS3^{hmin} in 0.5 ml subcutaneously and boosted with the same dose on day 30. On day 60, the macaques were challenged with 5 x 10^5 FFU NGC-44 in 0.5 ml delivered subcutaneously and euthanized on day 90. Blood samples were collected for virus titration by qRT-PCR on days 1–9 and 61–69, and for titration of neutralizing antibodies in sera on days 0, 15, 30, 60, 75, and 90.

2.6. Immunization and challenge of rhesus macaques

All animals were tested for dengue antibodies by ELISA and FRNT50 30 days before they were selected for the study. For these tests, 4 ml of blood was collected in SST tubes. For animal safety, CBC (2 ml EDTA tube) and chemistry (2 ml SST tube) was performed at baseline and at days 6, 15 and 30 after infection.

The immunogenicity of our vaccine candidates E^{hmin} and NS3^{hmin} was compared to synthetic wildtype DENV2^{syn} using rhesus macaques (*Macaca mulatta*). Briefly, 3-4-year-old male macaques (n = 6) were vaccinated in the upper arm with 0.5 mL containing 1 x 10^6 FFU of a vaccine candidate or DENV2^{syn}. A fourth control group was mock vaccinated and used to assess vaccine efficacy. Monkeys were vaccinated at day 0, bled for viremia measurement on days 1–9 and 61–69, and bled for neutralizing antibody detection at day 15, 30, 60, 75, and 90. Each macaque was boosted with the same dose of virus on day 30 (Fig. 2). Sera from day 15, 30, 60, and 90 taken from DENV2^{syn}, E^{hmin}, and NS3^{hmin} vaccinated macaques as well as day 90 sera from unvaccinated macaques were tested for neutralizing antibodies using a FRNT50 assay in Vero cells. At 60 days we challenged with 5 x 10^5 FFU DENV2 NGC-44 and collected serum for the next 10 days to monitor viremia by qRT-PCR.

2.7. DENV ELISA

Before conducting vaccination studies, we characterized the macaques' immune response against DENV and ZIKV to confirm that all animals did not have prior exposure. Seroreactivity to DENV was tested using commercial IgG and IgM ELISA kits (Focus, Cypress, CA). After vaccination, anti-DENV IgG, IgM levels as well as anti-NS1 IgG was examined using a commercial kit (Alpha Diagnostic, San Antonio, TX).

2.8. DENV RT-PCR

Viral RNA from serum samples was extracted using QIAmp Viral RNA mini kit (Qiagen, Valencia, CA) according to manufacturer instructions. Real-time RT-PCR (TaqMan) singleplex assay was performed using specific primers and probes for DENV2: Forward (5′ CAG GTT ATG GCA CTG TCA CGA T 3′), Reverse (5′ CCA TCT GCA GCA ACA CCA TCT C 3′) and Probe (5′ CTC TCC GAG AAC AGG CCT CGA CTT CAA 3′ HEX/BHQ1) (Sigma-Aldrich) were used. RNA from known full-length *in vitro* transcribed DENV2^{syn} was included as positive control. For the reaction mixture, 10 µL of RNA was combined with 100 µM primers and probes in a 50 µL total volume using qScript™ One-Step qRT-PCR master mix kit (Quanta Biosciences™) according to manufacturers' instructions. Thermocycling parameters were as follows: Reverse transcription for 30 min at 50 °C and reverse transcriptase inactivation for 12.5 min at 95 °C was followed by 45 cycles of 95 °C for 15 s and annealing at 60 °C for 1 min using the iCycler IQ5 Real Time Detection System (Optical System software version 2.1; Bio Rad, CA)(Johnson et al., 2005).

3. Results

3.1. Generation of DENV2 vaccine candidates

Our DENV vaccine candidates were based on wild-type dengue type 2 virus 16681 that we have synthesized *de novo* as described previously (Shen et al., 2015). We chose the coding regions E and NS3 for individual codon pair deoptimization with respect to *human* codon pair bias, as previously described (Shen et al., 2015) (Fig. 1A) and recoded them to reduce codon pair scores for human host systems while maintaining mosquito CPB (Fig. 1A, Table 1). Because the NS5^{hmin} virus is too highly attenuated in mice and barely viable in primate cell culture (Shen et al., 2015) we decided to focus on testing the E^{hmin} and NS3^{hmin} in non-human primates.

Generally, DENV does not cause overt diseases in non-human primates. The protocol to assess the effect of a DENV vaccine candidate, therefore, relies on the vaccine candidate's ability to induce immunity and prevent viremia in a vaccinated animal after subsequent challenge (Sariol and White, 2014).

Considering our previous results in neonatal mice (Shen et al., 2015), we tested three viruses in nonhuman primates: (1) The synthetic wild type strain DENV2^{syn} (Shen et al., 2015), (2) E^{hmin} and (3) NS3^{hMin} (the latter being the most highly attenuated variant in neonatal mice that replicated in cultured primate cells). Attenuation was measured by following viral replication through viremia (genome equivalents/ml) in vaccinated macaques. Immunogenicity of each candidate was tested using serum neutralizing antibody titers and DENV2-specific IgM and IgG levels post-vaccination. Efficacy was determined by measuring serum viremia post-challenge with DENV2 NGC-44. To these ends, rhesus macaques were vaccinated with 10^6 FFU on day 0 and boosted on day 30 with DENV2^{syn}, E^{hmin}, or NS3^{hmin}, or mock vaccinated subcutaneously (Fig. 2). On days 0–9 the macaques were tested for viremia from each vaccinating virus by qRT-PCR using primers annealing to common non-deoptimized sequence in each virus (Stauft et al., 2018). On day 60, each animal was challenged with 5 × 10^5 PFU of DENV2 NGC-44 and blood collected daily for 10 days to check for viremia by qRT-PCR. Sera were collected from each monkey on days 15, 30, 60, 75, and 90 for detection of neutralizing antibodies by FRNT50 assays in

Table 2
Neutralizing serum titers against DENV2^{syn} and DENV2 NGC-44.

RMID	Day 0		Day 15		Day 30		Day 60	
	DENV2^{syn}	NGC-44	DENV2^{syn}	NGC-44	DENV2^{syn}	NGC-44	DENV2^{syn}	NGC-44
Mock								
5O8	< 20	< 20	ND	ND	ND	ND	ND	ND
0P1	< 20	< 20	ND	ND	ND	ND	ND	ND
7O5	< 20	< 20	ND	ND	ND	ND	ND	ND
BS97	< 20	< 20	ND	ND	ND	ND	ND	ND
4PO	< 20	< 20	ND	ND	ND	ND	ND	ND
1O1	< 20	< 20	ND	ND	ND	ND	ND	ND
DENV2^{syn}								
1L0	< 20	< 20	20480	ND	5974	2560	4267	1280
CB20	< 20	< 20	10240	ND	5120	2560	2560	640
3N6	< 20	< 20	10240	ND	10240	2560	10240	1280
CB19	< 20	< 20	5120	ND	5120	640	2987	1280
0O0	< 20	< 20	7680	ND	5120	640	7680	1280
4L2	< 20	< 20	20480	ND	8534	5120	5120	2560
E^{hmin}								
BZ50	< 20	< 20	20	ND	40	20	80	20
BS29	< 20	< 20	20	ND	80	< 20	120	< 20
IK9	< 20	< 20	< 20	ND	< 20	< 20	40	< 20
1N6	< 20	< 20	40	ND	40	20	160	< 20
BS27	< 20	< 20	20	ND	160	< 20	2032	320
BZ49	< 20	< 20	30	ND	40	< 20	2032	160
NS3^{hmin}								
BS10	< 20	< 20	< 20	ND	< 20	< 20	40	< 20
8P1	< 20	< 20	< 20	ND	< 20	< 20	20	< 20
CB18	< 20	< 20	< 20	ND	< 20	< 20	< 20	< 20
BS26	< 20	< 20	< 20	ND	< 20	< 20	20	< 20
1M7	< 20	< 20	< 20	ND	< 20	< 20	< 20	< 20
CB43	< 20	< 20	< 20	ND	< 20	< 20	60	< 20

Neutralization of dengue 2 virus strains DENV2^{syn} (derived from DENV2 16681) and DENV2 NGC-44 in Vero cells in the presence of sera collected from mock vaccinated macaques or macaques vaccinated and booted with 1 x 10^6 FFU of DENV2^{syn}, E^{hmin}, NS3^{hmin} at baseline, day 15, day 30, and day 60 (30 days post boost). ND: Not done.

Vero cells against DENV2^{syn} or the challenge strain NGC-44 (Table 2).

Interestingly, no detectable viremia was present following vaccination with either deoptimized virus (Fig. 3) while viremia in DENV2^{syn} infected animals was detected starting on day 2 through day 8, with peak viremia observed on days 5–7. This corroborates our previous findings in human and non-human primate cell lines as well as neonatal mice (Shen et al., 2015; Stauft et al., 2018) with E^{hmin} and NS3^{hmin} showing a significant degree of selective attenuation (Shen et al., 2015; Stauft et al., 2018).

At 60 days post-vaccination and 30 days post-boost, 100% of DENV2^{syn} and E^{hmin} and 67% of NS3^{hmin} vaccinated monkeys seroconverted against homologous DENV2^{syn} (Table 2). Geometric mean FRNT$_{50}$ titers were lower in E^{hmin} (251.6) and NS3^{hmin} (31.4)

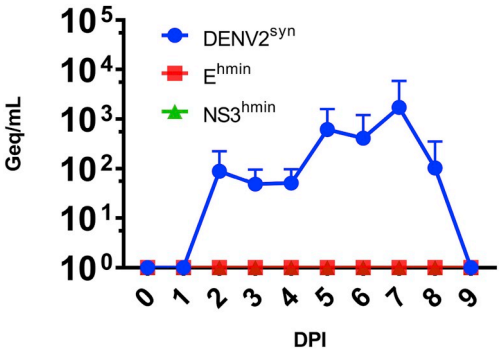

Fig. 3. E^{hmin} and NS3^{hmin} are highly attenuated in rhesus macaques. Viremia was quantified in vaccinated macaques (n = 6) 0–9 days post-vaccination with 10^6 FFU DENV2^{syn}, E^{hmin}, and NS3^{hmin} using qRT-PCR with DENV2 backbone specific primers to measure attenuation. DENV2^{syn} viremia titers peaked on days 5–7 while no detectable viremia was observed for either E^{hmin} or NS3^{hmin} vaccinated macaques.

vaccinated monkeys compared to DENV2^{syn} inoculated monkeys (4857.6) indicating that the attenuated viruses induced a less robust immune response (Table 2). Sera were also tested against a different strain of dengue 2 virus, NGC-44, which was used to challenge the vaccinated macaques. Overall, titers against NGC-44 were ~4–8 times lower than the FRNT$_{50}$ titers observed against DENV2^{syn}. This resulted in substantially lower seroconversion rates for E^{hmin} (50%) and NS3^{hmin} (0%) to DENV2 NGC-44.

In addition to neutralizing antibodies, levels of dengue 2-specific binding IgM (Fig. 4A) were tested by ELISA on days 5, 10, and 15 (post primary inoculation) as well as on days 35, 40, and 45 (5, 10, and 15 days post-boost, respectively) and compared using Dunnett's multiple comparison test in GraphPad Prism 7.0. After primary inoculation, DENV2^{syn} inoculated macaques reached high levels of serum dengue-specific IgM by 10 days post-infection, however, IgM levels remained low for E^{hmin} and NS3^{hmin} inoculated macaques until a second dose was administered on day 30. Significant increases in DENV2-specific serum IgM levels were observed in E^{hmin} vaccinated macaques on days 40 ($p = 0.0328$) and 45 ($p = 0.0357$). In NS3^{hmin} vaccinated macaques, DENV2-specific serum IgM levels increased significantly on days 40 ($p = 0.0001$), 45 ($p = 0.0406$), and 60 ($p = 0.0001$). Serum dengue-specific IgG (Fig. 4B) antibodies in inoculated macaque sera were tested as well, with all animals except one NS3^{hmin} vaccinated animal scoring positive 30 days post vaccination with a single dose. Elevated DENV2-specific IgM and IgG levels indicate immunogenicity post-boost with E^{hmin} and NS3^{hmin} despite low FRNT$_{50}$ values. In future studies we intend to characterize the nature of antibodies raised to vaccination with CPD DENV and determine whether the presentation of neutralizing epitopes differs in recoded viruses.

Because antibodies to the secreted form of the DENV NS1 protein have been shown to be protective in mouse models of DHF (Amorim et al., 2012; Beatty et al., 2015; Wu et al., 2003) and YFV NS1

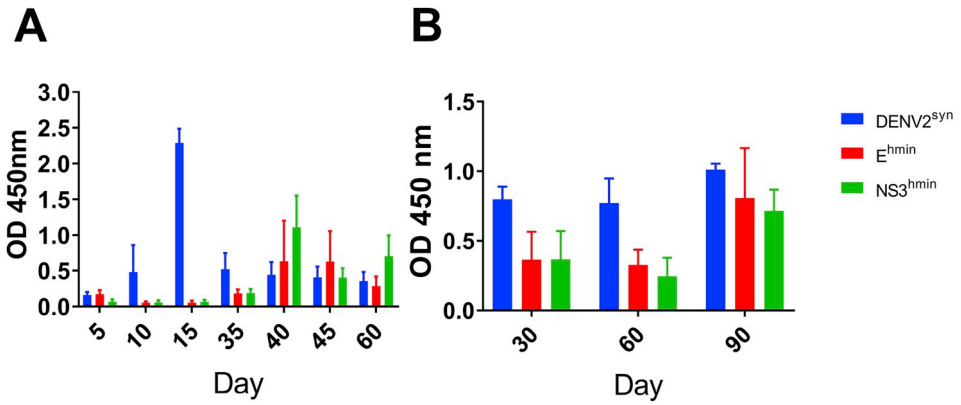

Fig. 4. Antibody responses to vaccination in rhesus macaques. (A) Dengue-specific IgM values days 0–60 post-vaccination and (B) IgG values at days 30, 60, and 90 (30 days post-challenge) for mock, DENV2^{syn}, E^{hmin}, and NS3^{hmin} vaccinated macaque sera were measured by ELISA.

vaccination has also been shown to be protective in macaques (Schlesinger et al., 1986), we tested our vaccinated macaques for antibodies against the NS1 protein (S1 Fig). Possibly due to the attenuated nature of our vaccines, only one E^{hmin} vaccinated animal had detectable anti-NS1 antibodies while all macaques in the DENV2^{syn} vaccinated group had anti-NS1 IgG at 60 days post vaccination (30 days post-boost). No NS3^{hmin} vaccinated animals developed detectable IgG against NS1 (S1 Fig).

On day 60 post-vaccination each macaque was challenged with DENV2 NGC-44 to test the protective effects of vaccination with CPD DENV2. Protection was assayed by testing the levels of NGC-44 viremia for 10 days' post-challenge in vaccinated macaques compared to the mock-vaccinated control group. Macaques with a FRNT$_{50}$ level of 160 or higher against NGC-44 (Table 2) did not show any viremia after challenge which included all the DENV2^{syn} inoculated animals and 33% (2/6) of E^{hmin} vaccinated macaques (Table 3). The onset of viremia was acute, with viral RNA detectable in the serum of mock vaccinated macaques on day 1 (4/6 animals) and all mock-vaccinated macaques were viremic on day 2 post-challenge. In macaques vaccinated with E^{hmin} and NS3^{hmin}, however, the onset of viremia was delayed with the majority of animals becoming viremic on day 2 or later post-challenge. In all animals, viremia was absent by day 7 post-challenge (Table 3). The average duration of viremia for E^{hmin} vaccinated macaques (3.17 days) was also shorter compared to mock vaccinated controls (4.5 days). This is due to the absence of viremia in animals BS27 and BZ49 and the difference in duration was not significant by Student's T-test ($p = 0.2432$). The average duration of viremia for NS3^{hmin} vaccinated macaques (4.67 days) was not different from the duration of viremia for mock vaccinated controls (Table 2). Peak viremia occurred earlier in mock-vaccinated animals compared to both E^{hmin} and NS3^{hmin} vaccinated groups indicating a delay from 2.17 days to 4.25 (E^{hmin}) or 4.33 days (NS3^{hmin}). Overall, the peak titer of viremia, measured in log$_{10}$

Table 3
DENV2 NGC-44 viremia post-challenge.

RMID	Viremia (log$_{10}$ genome copies/ml)										Peak Viremia (Day)	Total Days
	1	2	3	4	5	6	7	8	9	10		
Mock												28
5O8	4.49	5.16	4.66	4.39	3.05	–	–	–	–	–	2	
0P1	3.47	3.92	4.41	4.24	3.11	–	–	–	–	–	3	
7O5	3.12	4.58	4.18	3.76	3.33	–	–	–	–	–	2	
BS97	–	4.06	3.94	3.47	2.78	–	–	–	–	–	2	
4PO	4.30	4.76	3.84	4.37	3.26	–	–	–	–	–	2	
1O1	–	4.27	–	3.58	3.49	2.23	–	–	–	–	2	
DENV2^{syn}												0
1L0	–	–	–	–	–	–	–	–	–	–		
CB20	–	–	–	–	–	–	–	–	–	–		
3N6	–	–	–	–	–	–	–	–	–	–		
CB19	–	–	–	–	–	–	–	–	–	–		
0O0	–	–	–	–	–	–	–	–	–	–		
4L2	–	–	–	–	–	–	–	–	–	–		
E^{hmin}												20
BZ50	–	2.84	4.82	5.37	5.35	2.97	–	–	–	–	4	
BS29	1.81	3.41	3.69	2.60	3.25	–	–	–	–	–	3	
IK9	2.25	–	2.00	1.87	4.48	4.26	–	–	–	–	5	
1N6	–	2.91	3.42	2.94	4.14	3.42	–	–	–	–	5	
BS27	–	–	–	–	–	–	–	–	–	–		
BZ49	–	–	–	–	–	–	–	–	–	–		
NS3^{hmin}												28
BS10	–	3.55	3.86	4.71	4.62	3.18	–	–	–	–	4	
8P1	–	3.77	3.19	4.03	4.10	2.87	–	–	–	–	5	
CB18	–	3.93	3.25	4.30	4.32	3.61	–	–	–	–	5	
BS26	–	3.59	3.60	3.24	4.32	3.01	–	–	–	–	5	
1M7	–	–	1.94	3.28	3.11	2.89	–	–	–	–	4	
CB43	1.56	3.17	4.20	4.00	–	–	–	–	–	–	3	

-: below limit of detection.

genome equivalents/mL, was not significantly different between either E^{hmin} or $NS3^{hmin}$ vaccinated macaques compared to mock vaccinated controls. However, the viremia on day 2 was significantly higher in mock-vaccinated macaques than those receiving E^{hmin} or $NS3^{hmin}$ ($p = 0.0031$ and $p = 0.0037$ respectively).

3.2. Modified recoding of deoptimized DENV to adjust attenuation

Based on our previous E^{hmin} construct, we shortened the CPD region within E^{hmin} gene (Fig. 2) to generate two separate E^{hmin} variants named E^{hminA} and E^{hminB}, which we predicted would be less attenuated ("de-attenuated"). Relative to wildtype E, E^{hminA} and E^{hminB} in these subcloned vaccine candidates contained 156- and 178-point mutations, respectively (Table 1). E E^{hminA} and E^{hminB}were tested for attenuation *in vitro* using growth kinetics and spread by focus-forming unit (FFU) size (S2 Fig) in primate Vero and LLC-MK2 cells as well as by comparative titers in C6/36 cells. Viral stocks of $DENV2^{syn}$, E^{hmin}, E^{hminA}, and E^{hminB} were initially grown in permissive mosquito (C6/36; *Aedes albopictus*) cells then titrated in parallel by FFA in C6/36 and Vero cell lines (S2 Fig). Comparison of relative titer and focus forming unit size at 6 days post infection (dpi) show that all viruses replicated to comparable yields in mosquito C6/36 cells. In primate-derived Vero and LLC-MK2 cells, E^{hminA} and E^{hminB} exhibited an intermediate FFU size phenotype between E^{hmin} and $DENV2^{syn}$. Unexpectedly, E^{hminB} demonstrated a smaller FFU phenotype in Vero cells compared to E^{hminA} even though the number of nucleotide mutations, the codon pair score (CPS), and increased numbers of CpG dinucleotides are similar for both sub-cloned variants (Table 1). However, FFU size increase was observed with an increasing proportion of wild-type CPB in the order $E^{hmin} < E^{hminB} < E^{hminA} < DENV2^{syn}$ (S2 Fig).

We compared stock virus titers between Vero (primate) and C6/36 (mosquito) cells. E^{hminA} had the highest Vero to C6/36 ratio (2.7-fold, $p = 0.0002$), DENV2syn the next highest (slightly greater than 1, $p = 0.205$), E^{hminB} the next highest (ratio of 1) albeit with small FFU size in Vero cells, and E^{hmin} titer was significantly lower by ~20-fold ($p = 0.0006$) (S3 Fig) in Vero cells. Following pilot experiments with titrated stocks, further confirmation of an intermediate E^{hminA} and E^{hminB} phenotype compared to $DENV2^{syn}$ and E^{hmin} was investigated in primate Vero and LLC-MK2 cells using single-step growth kinetics after infection at 1 MOI (Fig. 5A/B). In both cell lines, $DENV2^{syn}$ and E^{hminA} had the fastest growth, and were very similar to each other. E^{hminB} grew slightly more slowly, while E^{hmin} grew even more slowly, and plateaued at a lower final titer (Fig. 5). Overall, increased replication in primate cells was observed with increased human CPS in each virus, in the order $E^{hmin} < E^{hminB} < E^{hminA} = DENV2^{syn}$. Overall, the reduction of CPD increased replication of E^{hminA} and E^{hminB} in mammalian cells but had little if any effect in mosquito cells, as expected.

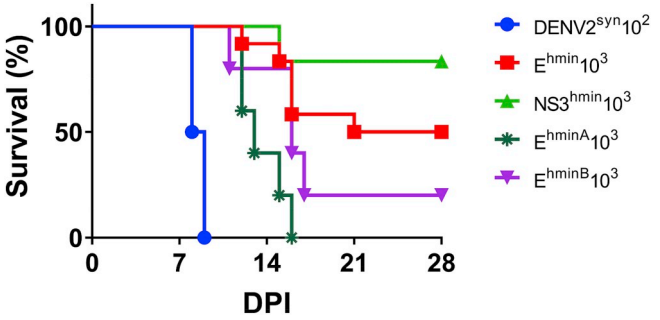

Fig. 6. Intermediate attenuation in neurovirulence for neonatal Swiss Webster mice was observed in viruses with reduced CPD sequence. Kaplan-Meier survival curves indicate that E^{hminA} and E^{hminB} are less virulent than $DENV2^{syn}$ at doses of 10^3 FFU (compared to 10^2 FFU dose with $DENV2^{syn}$) while also more virulent than the E^{hmin}, and $NS3^{hmin}$ viruses at the same dose.

3.3. Attenuation of subcloned deoptimized variants in neonatal mice

To confirm attenuation of the subcloned deoptimized variants *in vivo* we tested them for neurovirulence in a neonatal Swiss Webster mouse model of infection (Fig. 6). The methods used to measure virulence were mean-time-to-death (MTD), lethal dose 50% (LD50), and comparison of survival kinetics. For these experiments, humane early-endpoints were used in lieu of mortality (outlined in methods). As seen in primate cell culture, the sub-cloned E^{hminA} was similar in virulence to $DENV2^{syn}$ in terms of LD_{50} but with a significantly extended MTD (13.6 days versus 8.5 days). Nevertheless, differing Kaplan-Meier survival kinetics ($p = 0.0020$ Mantel-Cox test, GraphPad Prism 7.0) at a dose of 10^2 FFU indicated some measure of attenuation. Compared to E^{hminA}, the LD_{50} of E^{hmin} was ≥1000-fold higher (Table 4), with a slightly higher MTD (14.75 days versus 13.6 days) and differing Kaplan-Meier survival kinetics ($p = 0.0404$ Mantel-Cox test, GraphPad Prism 7.0) compared in neonates infected i.c. with 10^3 FFU of either virus (Fig. 6). The E^{hminB} virus was more attenuated in neonatal Swiss Webster mice than either $DENV2^{syn}$ or E^{hminA}, with 10-fold higher LD_{50} values (Table 4) and intermediate Kaplan-Meier survival kinetics in mice infected with a dose of 10^3 FFU (Fig. 6). Thus, division of the CPD region resulted in viruses with an intermediate neurovirulence phenotype in newborn mice which are highly sensitive to intracranial injection with DENV2.

4. Discussion

Selective viral attenuation by means of codon-pair deoptimization was reported for the first time by us (Shen et al., 2015) and is being used by our lab to construct vaccine candidates for arboviruses like DENV, chikungunya, and Zika viruses. While there has been a lively

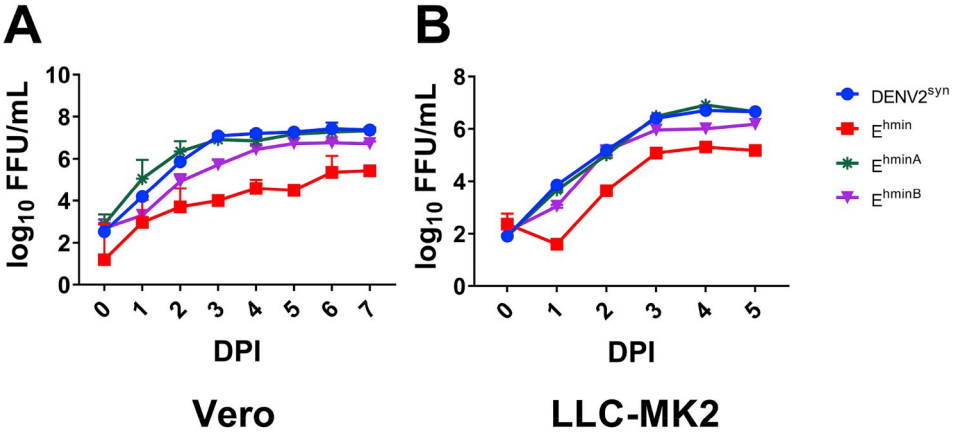

Fig. 5. Attenuation in primate cell culture is related to length of deoptimized sequence. (A) Vero and (B) LLC-MK2 cells were infected at an MOI of 1.0 with $DENV2^{syn}$, E^{hmin}, or the sub-cloned E^{hminA} and E^{hminB} containing ½ deoptimized E^{hmin} sequence and ½ wt sequence for the E glycoprotein encoding region. Growth kinetics at 37 °C show that the sub-cloned viruses exhibit an intermediate phenotype in primate cells.

Table 4
MTD and LD50 values in neonatal Swiss Webster mice injected i.c.

Virus	MTD	LD50 (FFU)
$DENV2^{syn}$	8.5*	3.2
E^{hminA}	13.6	10
E^{hminB}	15	52
E^{hmin}	16	1200
$NS3^{hmin}$	15	≥2500

*Dose is 10^2 FFU.

debate as to the exact mechanism by which CDP vaccine candidates are attenuated (Futcher et al., 2015), attenuation by codon pair deoptimization has been shown *in vivo* with such disparate human viruses such as dengue virus (Shen et al., 2015; Stauft et al., 2018), poliovirus (Coleman et al., 2008; Song et al., 2017), respiratory syncytial virus (RSV) (Le Nouën et al., 2014; Nouën et al., 2017), Influenza A virus (Broadbent et al., 2016; Kaplan et al., 2018; Yang et al., 2013), and vesicular stomatitis virus (Wang et al., 2015). CPD has been applied also towards HIV (Martrus et al., 2013) and viruses important in veterinary medicine as well, with success in foot and mouth disease virus (FMDV) (Diaz-San Segundo et al., 2015), porcine reproductive and respiratory syndrome virus (PRRSV) (Ni et al., 2014), and Marek's disease virus (Conrad et al., 2018; Eschke et al., 2018).

Of note, our $DENV2^{syn}$ was immunogenic in rhesus macaques against itself ($DENV2^{syn}$) but also the heterologous DENV2 NGC-44 similar to what has been observed with wild-type dengue 2 16681 in previous experiments (Sariol and White, 2014). Viremia after $DENV2^{syn}$ occurred in each infected macaque on day 2 post-infection but was undetectable in E^{hmin} or $NS3^{hmin}$ vaccinated animals thereby confirming the attenuation of our vaccine candidates *in vivo*. For our study we chose to challenge the macaques with the more virulent DENV2 strain NGC-44, which causes higher levels of viremia in Rhesus macaques and to test for the breadth of cross-neutralization among different DENV2 genotypes. We found that neutralizing antibody titers were higher against the homologous DENV2 16681 (Asian I genotype) (Galula et al., 2014) strain compared to the NGC-44 strain, which belongs to a different genotype (AS-II) (Añez et al., 2011) of DENV2 virus. It is our opinion that the vaccine candidates were too attenuated to be properly immunogenic against multiple genotypes of DENV2 and, based on FRNT50 results (Table 2) it is possible that better protection would have been observed with DENV2 16681 challenge. However, the significant delay in the peak viremia after challenge, the lower peak viremia at day 2 post-challenge, and the observed increase in neutralizing and DENV-specific antibodies after vaccination with E^{hmin} or $NS3^{hmin}$ confirm the potential of these attenuated vaccine candidates. Additionally, although the 50% end-point was not reached in some E^{hmin} and $NS3^{hmin}$ vaccinated macaques, some DENV2 NGC-44 neutralization was observable at low dilutions of serum (S4 Fig). This may explain the delayed viremia post-challenge (Table 3).

Similar to our previous results with poliovirus (Coleman et al., 2008), the attenuation of CDP can be tuned by either adjusting the score of two genomic sequences with a similar number of mutations (E^{hmin} versus $NS3^{hmin}$) or through the use of subcloning to reduce the length of the deoptimized sequence as was done to make E^{hminA} and E^{hminB}. Subcloning produced viruses intermediate in phenotype between the wild-type $DENV2^{syn}$ and the highly attenuated E^{hmin} which should hopefully improve the immunogenicity of our candidates in future non-human primate studies with E^{hminA} and E^{hminB}. We will also apply this strategy to future vaccine development with the closely related ZIKV and other emerging flaviviruses. Through fine adjustment of selective deoptimization, it should be possible to produce vaccine candidates with the right balance of selective attenuation and potent immunogenicity.

These results confirm the foundation of our strategy to generate viruses with reduced virulence: it varies with the extent of codon pair deoptimization. This takes into account the size of the viral genome and the average codon pair score - how many disfavored codon pairs were introduced into the recoded viral genome sequence. We consider the correlation between recoding and attenuation to be *proof of concept* of our strategy to study proliferation and virulence of RNA viruses. We have shown that the attenuation of DENV2 vaccine candidates *in vitro* and *in vivo* can be adjusted by simply changing the length of recoded portions of the genome. Interestingly, E^{hminA} and E^{hminB} had significantly different attenuation phenotypes *in vitro* and *in vivo* despite similar numbers of mutations (and C_3G_1 frequency) but were both still intermediate between $DENV2^{syn}$ and E^{hmin} in terms of virulence.

Both E^{minA} and E^{minB} will be tested in future experiments with non-human primates. It may be necessary to include into our studies vaccine candidates with partially recoded NS3 as well.

5. Ethics statement

All mouse experiments conducted in this study were approved by the Stony Brook University Institutional Animal Care and Use Committee (IACUC) under protocol number 606687 using guidelines from *Guide for the Care and Use of Laboratory Animals*, 8th Edition. Mouse experiments were conducted at the Office of Laboratory Animal Welfare accredited Division of Laboratory Animal Resources at Stony Brook University (OLAW Assurance #: D16-00006).

Young adult rhesus macaques (3–4 years of age) seronegative for DENV and ZIKV were housed in the Caribbean Primate Research Center (CPRC) facilities, University of Puerto Rico, San Juan, Puerto Rico. All procedures were reviewed and approved by the Institute's Animal Care and Use Committee at Medical Sciences Campus, University of Puerto Rico (IACUC-UPR-MSC), and performed in a facility accredited by the Association for Assessment and Accreditation of Laboratory Animal Care (AAALAC) (Animal Welfare Assurance number A3421; protocol number, 7890215). In addition, steps were taken to ameliorate suffering in accordance with the recommendations of the Weatherall report on The Use of Nonhuman Primates in Research (Weatherall, 2006). For instance, all procedures were conducted under anesthesia by intramuscular injection of ketamine at 10–20 mg kg^{-1} of body weight, as approved by the IACUC. Anesthesia was delivered in the caudal thigh using a 23-Gauge sterile syringe needle. During the period of the entire study, the macaques were under the environmental-enrichment program of the facility, also approved by the IACUC. Macaques were continuously monitored by trained veterinarians at the Animal Research Center. During the execution of this project animals were infected in groups of 6.

Funding

This work was supported in part by NIH grant AI110792-01A1 (to EW), NIH grant 1R21AI126048-01 (to Y.S.), R01 GM119175 (BF), and NIH grants 2P40 OD012217 and 2U42OD021458-15 to CAS (ORIP, OD, NIH).

Authors' contributions

CBS was responsible for the generation and analysis of experimental results as well as drafting the report. YS contributed equally by conducting experiments and writing the report. OG conducted data analysis and figure preparation. EA provided technical advice and assisted in figure preparation. PP generated experimental data. BF assisted in manuscript preparation and experimental design. IVR coordinated and assisted in the conduct of non-human primate experiments. CAS was responsible for directing the non-human primate studies, provided technical advice, analyzed the NHP results as well as reviewing the manuscript. EW was responsible for directing and coordinating the project as well as planning, designing, and reviewing the results of the study and directing manuscript preparation. All authors had full access

to the data generated from this study, assisted in the writing of this report, and are responsible for the decision to submit this report for publication.

Conflicts of interest

EW is a co-founder and consultant of Codagenix, Inc., and CS is currently employed by Codagenix, Inc., a commercial company that is developing vaccines based on recoded viruses. There are no new patents, products in development or marketed products to declare. This does not alter our adherence to all the Vaccine journal policies on sharing data and materials.

Acknowledgements

We thank the dedicated staff at Cayo Santiago, Sabana Seca Field Station and the Animal Resources Center for their continued dedication and care in support of the CPRC's animal population. We also thank the staff at the Virology Laboratory, Medical Sciences Campus, UPR for their commitment with this work. JoAnn Mugavero's competent help in all aspects of this work and Jeronimo Cello's discussions are highly appreciated.

Appendix A. Supplementary data

Supplementary data to this article can be found online at https://doi.org/10.1016/j.virol.2019.09.003.

References

Amorim, J.H., Diniz, M.O., Cariri, F.A.M.O., Rodrigues, J.F., Bizerra, R.S.P., Gonçalves, A.J.S., de Barcelos Alves, A.M., de Souza Ferreira, L.C., 2012. Protective immunity to DENV2 after immunization with a recombinant NS1 protein using a genetically detoxified heat-labile toxin as an adjuvant. Vaccine 30, 837–845. https://doi.org/10.1016/j.vaccine.2011.12.034.

Añez, G., Morales-Betoulle, M.E., Rios, M., 2011. Circulation of different lineages of dengue virus type 2 in Central America, their Evolutionary time-scale and selection pressure analysis. PLoS One 6. https://doi.org/10.1371/journal.pone.0027459.

Beatty, P.R., Puerta-Guardo, H., Killingbeck, S.S., Glasner, D.R., Hopkins, K., Harris, E., 2015. Dengue virus NS1 triggers endothelial permeability and vascular leak that is prevented by NS1 vaccination. Sci. Transl. Med. 7 304ra141-304ra141. https://doi.org/10.1126/scitranslmed.aaa3787.

Broadbent, A.J., Santos, C.P., Anafu, A., Wimmer, E., Mueller, S., Subbarao, K., 2016. Evaluation of the attenuation, immunogenicity, and efficacy of a live virus vaccine generated by codon-pair bias de-optimization of the 2009 pandemic H1N1 influenza virus, in ferrets. Vaccine 34, 563–570. https://doi.org/10.1016/j.vaccine.2015.11.054.

Cello, J., Paul, A.V., Wimmer, E., 2002. Chemical synthesis of poliovirus cDNA: generation of infectious virus in the absence of natural template. Science 297, 1016–1018. https://doi.org/10.1126/science.1072266.

Coleman, J.R., Papamichail, D., Skiena, S., Futcher, B., Wimmer, E., Mueller, S., 2008. Virus attenuation by genome-scale changes in codon pair bias. Science 320, 1784–1787. https://doi.org/10.1126/science.1155761.

Conrad, S.J., Silva, R.F., Hearn, C.J., Climans, M., Dunn, J.R., 2018. Attenuation of Marek's disease virus by codon pair deoptimization of a core gene. Virology 516, 219–226. https://doi.org/10.1016/j.virol.2018.01.020.

Diaz-San Segundo, F., Medina, G.N., Ramirez-Medina, E., Velazquez-Salinas, L., Koster, M., Grubman, M.J., de Los Santos, T., 2015. Synonymous deoptimization of foot-and-mouth disease virus causes attenuation in vivo while inducing a strong neutralizing antibody response. J. Virol. 90, 1298–1310. https://doi.org/10.1128/JVI.02167-15.

Eschke, K., Trimpert, J., Osterrieder, N., Kunec, D., 2018. Attenuation of a very virulent Marek's disease herpesvirus (MDV) by codon pair bias deoptimization. PLoS Pathog. 14, e1006857. https://doi.org/10.1371/journal.ppat.1006857.

Futcher, B., Gorbatsevych, O., Shen, S.H., Stauft, C.B., Song, Y., Wang, B., Leatherwood, J., Gardin, J., Yurovsky, A., Mueller, S., Wimmer, E., 2015. Reply to Simmonds et al.: codon pair and dinucleotide bias have not been functionally distinguished. Proc. Natl. Acad. Sci. U. S. A. 112, E3635–E3636. https://doi.org/10.1073/pnas.1507710112.

Galula, J.U., Shen, W.-F., Chuang, S.-T., Chang, G.-J.J., Chao, D.-Y., 2014. Virus-like particle secretion and genotype-dependent immunogenicity of dengue virus serotype 2 DNA vaccine. J. Virol. JVI. 00810–14. https://doi.org/10.1128/JVI.00810-14.

Gutman, G.A., Hatfield, G.W., 1989. Nonrandom utilization of codon pairs in Escherichia coli. Proc. Natl. Acad. Sci. 86, 3699–3703.

Johnson, B.W., Russell, B.J., Lanciotti, R.S., 2005. Serotype-specific detection of dengue viruses in a fourplex real-time reverse transcriptase PCR assay. J. Clin. Microbiol. 43, 4977–4983. https://doi.org/10.1128/JCM.43.10.4977-4983.2005.

Kaplan, B.S., Souza, C.K., Gauger, P.C., Stauft, C.B., Robert Coleman, J., Mueller, S., Vincent, A.L., 2018. Vaccination of pigs with a codon-pair bias de-optimized live attenuated influenza vaccine protects from homologous challenge. Vaccine 36, 1101–1107. https://doi.org/10.1016/j.vaccine.2018.01.027.

Le Nouën, C., Brock, L.G., Luongo, C., McCarty, T., Yang, L., Mehedi, M., Wimmer, E., Mueller, S., Collins, P.L., Buchholz, U.J., DiNapoli, J.M., 2014. Attenuation of human respiratory syncytial virus by genome-scale codon-pair deoptimization. Proc. Natl. Acad. Sci. U. S. A. 111, 13169–13174. https://doi.org/10.1073/pnas.1411290111.

Leary, S., Underwood, W., Anthony, R., Cartner, S., Golab, G.C., Patterson-Kane, E., 2013. AVMA Guidelines for the Euthanasia of Animals: 2013 Edition. pp. 102.

Li, P., Ke, X., Wang, T., Tan, Z., Luo, D., Miao, Y., Sun, J., Zhang, Y., Liu, Y., Hu, Q., Xu, F., Wang, H., Zheng, Z., 2018. Zika virus attenuation by codon pair deoptimization induces sterilizing immunity in mouse models. J. Virol. 92, e00701–18. https://doi.org/10.1128/JVI.00701-18.

Lindenbach, B.D., Murray, C., Thiel, H., Rice, C.M., n.d. Flaviviridae, in: Knipe, D., Howley, P. (Eds.), Fields Virology. Lippincott Williams & Wilkins, Philadelphia, p. 712.

Martrus, G., Nevot, M., Andres, C., Clotet, B., Martinez, M.A., 2013. Changes in codon-pair bias of human immunodeficiency virus type 1 have profound effects on virus replication in cell culture. Retrovirology 10 (78).

Mueller, S., Papamichail, D., Coleman, J.R., Skiena, S., Wimmer, E., 2006. Reduction of the rate of poliovirus protein synthesis through large-scale codon deoptimization causes attenuation of viral virulence by lowering specific infectivity. J. Virol. 80, 9687–9696. https://doi.org/10.1128/JVI.00738-06.

Mueller, S., Ping, P., Rieder, E., de Jesus, N., Iwasaki, A., Paul, A., Cello, J., Wimmer, E., 2005. Pathogenesis and prevention of poliomyelitis and the chemical synthesis of poliovirus. Nova Acta Leopoldina NF 92, 1–9.

Ni, Y.-Y., Zhao, Z., Opriessnig, T., Subramaniam, S., Zhou, L., Cao, D., Cao, Q., Yang, H., Meng, X.-J., 2014. Computer-aided codon-pairs deoptimization of the major envelope GP5 gene attenuates porcine reproductive and respiratory syndrome virus. Virology 450 (451), 132–139. https://doi.org/10.1016/j.virol.2013.12.009.

Nouën, C.L., McCarty, T., Brown, M., Smith, M.L., Lleras, R., Dolan, M.A., Mehedi, M., Yang, L., Luongo, C., Liang, B., Munir, S., DiNapoli, J.M., Mueller, S., Wimmer, E., Collins, P.L., Buchholz, U.J., 2017. Genetic stability of genome-scale deoptimized RNA virus vaccine candidates under selective pressure. Proc. Natl. Acad. Sci. 114, E386–E395. https://doi.org/10.1073/pnas.1619242114.

Pierson, T.C., Diamond, M.S., n.d. Flaviviruses, in: Knipe, D., Howley, P. (Eds.), Fields Virology. Lippincott Williams & Wilkins, Philadelphia, pp. 747–794.

Sariol, C.A., White, L.J., 2014. Utility, limitations, and future of non-human primates for dengue research and vaccine development. Front. Immunol. 5. https://doi.org/10.3389/fimmu.2014.00452.

Schlesinger, J.J., Brandriss, M.W., Cropp, C.B., Monath, T.P., 1986. Protection against yellow fever in monkeys by immunization with yellow fever virus nonstructural protein NS1. J. Virol. 60, 1153–1155.

Shen, S.H., Stauft, C.B., Gorbatsevych, O., Song, Y., Ward, C.B., Yurovsky, A., Mueller, S., Futcher, B., Wimmer, E., 2015. Large-scale recoding of an arbovirus genome to rebalance its insect versus mammalian preference. Proc. Natl. Acad. Sci. 112, 4749–4754. https://doi.org/10.1073/pnas.1502864112.

Song, Y., Gorbatsevych, O., Liu, Y., Mugavero, J., Shen, S.H., Ward, C.B., Asare, E., Jiang, P., Paul, A.V., Mueller, S., Wimmer, E., 2017. Limits of variation, specific infectivity, and genome packaging of massively recoded poliovirus genomes. Proc. Natl. Acad. Sci. 114, E8731–E8740. https://doi.org/10.1073/pnas.1714385114.

Stauft, C.B., Shen, S.H., Song, Y., Gorbatsevych, O., Asare, E., Futcher, B., Mueller, S., Payne, A., Brecher, M., Kramer, L., Wimmer, E., 2018. Extensive recoding of dengue virus type 2 specifically reduces replication in primate cells without gain-of-function in Aedes aegypti mosquitoes. PLoS One 13, e0198303. https://doi.org/10.1371/journal.pone.0198303.

Wang, B., Yang, C., Tekes, G., Mueller, S., Paul, A., Whelan, S.P.J., Wimmer, E., 2015. Recoding of the vesicular stomatitis virus L gene by computer-aided design provides a live, attenuated vaccine candidate. mBio 6. https://doi.org/10.1128/mBio.00237-15.

Weatherall, D., 2006. The Weatherall report on the use of non-human primates in research. Lond. R. Soc. 1–145.

Wu, S.-F., Liao, C.-L., Lin, Y.-L., Yeh, C.-T., Chen, L.-K., Huang, Y.-F., Chou, H.-Y., Huang, J.-L., Shaio, M.-F., Sytwu, H.-K., 2003. Evaluation of protective efficacy and immune mechanisms of using a non-structural protein NS1 in DNA vaccine against dengue 2 virus in mice. Vaccine 21, 3919–3929. https://doi.org/10.1016/S0264-410X(03)00310-4.

Yang, C., Skiena, S., Futcher, B., Mueller, S., Wimmer, E., 2013. Deliberate reduction of hemagglutinin and neuraminidase expression of influenza virus leads to an ultra-protective live vaccine in mice. Proc. Natl. Acad. Sci. U. S. A. 110, 9481–9486. https://doi.org/10.1073/pnas.1307473110.